

ELASTO-PLASTIC ANALYSIS OF PLATES
USING THE FINITE ELEMENT METHOD

Pål G. Bergan*

The Technical University of Norway, Trondheim

Ray W. Clough**

University of California, Berkeley

The formulation of a general quadrilateral finite element accounting for inelastic material behavior is described. Both flexural and membrane behavior are considered. The flow theory of plasticity is adopted, and the material is assumed to obey the von Mises yield criterion and the isotropic hardening law. Elasto-plastic problems are generally very costly in computer time, and emphasis is placed on an efficient formulation of the element stiffness. A pure incremental technique is chosen for the numerical solution procedure. Results are presented for various types of flexural and membrane plate problems. These examples demonstrate that the present method exhibits a high degree of accuracy while being highly efficient. It is concluded that the element described here is among the most versatile and efficient elasto-plastic elements yet devised.

*Associate Professor of Civil Engineering

**Professor of Civil Engineering

SECTION I

INTRODUCTION

Great advances were made in the field of plasticity during the 1940's and 1950's, and the development of the small deformation theory was essentially completed by the end of this period. However, solutions were then available only for a very limited number of simplified problems. The analysis of more complex problems was not possible until the advent of the electronic computer made numerical solution procedures practicable. The finite element method, which originally was applied to linear elastic systems, has proven also to provide one of the most effective numerical formulations for problems involving non-linear material behavior. Elasto-plastic finite element analyses have now been made of nearly every basic type of structural system, including plates, axisymmetric shells and solids, and general three-dimensional solids. References 1-6 are typical of the many papers describing such analyses.

The purpose of this paper is to describe the formulation and application of a highly efficient finite element for the analysis of elasto-plastic plates subjected simultaneously to in-plane and out-of-plane forces. Consideration is given here only to the incorporation of non-linear material effects in the analysis; however, the formulation could be extended without any essential difficulty to account for the non-linear effects of large displacements at the same time.

The organization of this paper follows the sequence of steps involved in the formulation of the finite element procedure. Consideration is given first to the constitutive law which expresses the non-linear relation between stresses and strains. In this work, the Prandtl-Reuss flow theory^[7], which assumes the increment of plastic strains to be proportional to the corresponding deviatoric stress components, is adopted because it seems the most consistent concept both mathematically and physically.

The next step in the formulation is establishing the strain distribution. This is the essential step of the finite element method and is embodied in the selection of the element displacement interpolation functions. Two types of displacement functions are employed in the quadrilateral element developed here: (1) the transverse bending displacements are expressed by the linear curvature compatible interpolation functions derived for the Q-19 plate bending element^[8], (2) the in-plane displacements are expressed by the bilinear interpolations of the plane isoparametric element family^[9]. The integration procedures used in computing the element stiffness have been modified from those of the cited references, however, in order to account for the variation of material properties within the element as a function of the strains.

The last step in the analysis is the formulation and solution of the equations of equilibrium. These equations reflect the non-linearity of the material properties, of course, and are solved in this work by an incremental tangent stiffness procedure. This approach has been selected in preference to the "initial stress" or "initial strain" methods because of its general reliability and its compatibility with the incremental flow theory of plasticity. (Comparisons between the two methods are presented in References 3, 6 and 10). The efficiency of the entire solution process is demonstrated by a series of examples at the end of the paper.

SECTION II

GOVERNING MATERIAL RELATIONS

Basic Assumptions and Material Laws

A short outline of the derivations leading to the mathematical expressions for the incremental stress-strain relationship will be given in the following. Proofs and details will not be included; more complete derivations may be found in References 3, 7, 11 and 12.

This derivation is based on three major assumptions. The first assumption is that the elastic and plastic strains may be additively decomposed

$$\epsilon_{ij} = \epsilon_{ij}^E + \epsilon_{ij}^P \quad (1)$$

where E and P denote "elastic" and "plastic" respectively. Both stresses and strains are referred to a rectangular Cartesian coordinate system. The strains are assumed to be infinitesimal (in fact, Equation 1 is not valid for finite strains). The plastic part of the strains is postulated to be incompressible:

$$\epsilon_{ii}^P = 0 \quad (2)$$

The second major assumption is that there exists a loading function f in 9-dimensional stress-space. $f = 0$ at time t constitutes the yield criterion at that time, $f > 0$ is inadmissible. As it turns out that f is a function of σ_{ij} and ϵ_{ij}^P , three different loading conditions from a plastic state ($f = 0$) result

$$\begin{aligned} \frac{\partial f}{\partial \sigma_{ij}} \dot{\sigma}_{ij} &< 0 && \text{(during unloading)} \\ \frac{\partial f}{\partial \sigma_{ij}} \dot{\sigma}_{ij} &= 0 && \text{(during neutral loading)} \\ \frac{\partial f}{\partial \sigma_{ij}} \dot{\sigma}_{ij} &> 0 && \text{(during loading)} \end{aligned} \quad (3)$$

The dot denotes time differentiation.

The material is further assumed to be stable as defined by Drucker^[11]. Drucker's postulate has three important implications, namely "convexity", "consistency" and "normality". Normality implies that at a regular point of the loading surface $f = 0$, the vector $d\epsilon_{ij}^P$ is in the direction of the outward normal to the yield surface (in stress space), so that

$$d\epsilon_{ij}^P = d\lambda \frac{\partial f}{\partial \sigma_{ij}} \quad (4)$$

$d\lambda$ is a non-negative scalar. When the material obeys the von Mises yield criterion (as will be assumed here), the flow rule of Eq. 4 is equivalent to the Prandtl-Reuss equation. By virtue of Eq. 4, the loading function plays the role of a plastic potential. f remains zero when going from one plastic state to another, hence

$$df = \frac{\partial f}{\partial \sigma_{ij}} d\sigma_{ij} + \frac{\partial f}{\partial \epsilon_{ij}^P} d\epsilon_{ij}^P = 0 \quad (5)$$

The initial yield criterion (von Mises) and the loading function are given by

$$f = \bar{\sigma} - T = \bar{\sigma} - k \sqrt{3} = 0 \quad (6)$$

where T is the initial yield stress in uniaxial tension, k is the yield stress in pure shear and $\bar{\sigma}$ is the equivalent stress given by

$$\bar{\sigma} = \sqrt{3J_2} = \sqrt{\frac{3}{2} s_{ij} s_{ij}} \quad (7)$$

in which J_2 is the second deviatoric-stress invariant and s_{ij} the deviatoric-stress components.

Further, it is assumed that the material exhibits an isotropic hardening behavior (Fig. 1). This implies a uniform expansion of the initial yield surface. The hardening is measured according to the plastic strain hypothesis (which is here equivalent to work hardening) and the yield criterion for subsequent yielding becomes

$$f = \bar{\sigma} - H(\bar{\epsilon}^P) = 0 \quad (8)$$

H is a function of the equivalent plastic strain $\bar{\epsilon}^P$ which is the integral of

$$d\bar{\epsilon}^P = \sqrt{\frac{2}{3}} \left\{ d\epsilon_{ij}^P d\epsilon_{ij}^P \right\}^{1/2} \quad (9)$$

As will be seen later, $H' = \frac{\partial H}{\partial \bar{\epsilon}^P}$ is of special interest and is easily obtainable from a uniaxial tension test curve, as shown in Fig. 2:

$$\frac{1}{H'} = \frac{1}{E_T} - \frac{1}{E} \quad (10)$$

E_T is the tangent modulus.

General Constitutive Equations

The following relation can be derived from Hooke's law and Equations 1, 4, 5 and 8^[11, 12]:

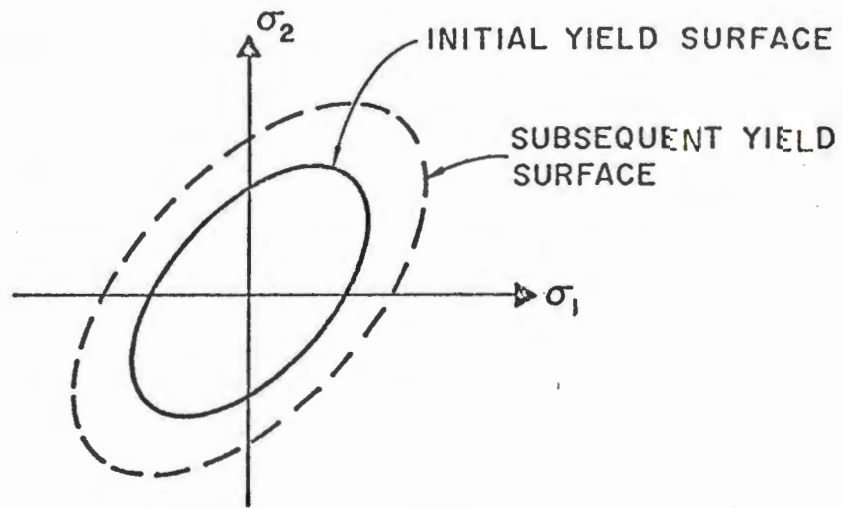


FIG. 1 ISOTROPIC HARDENING

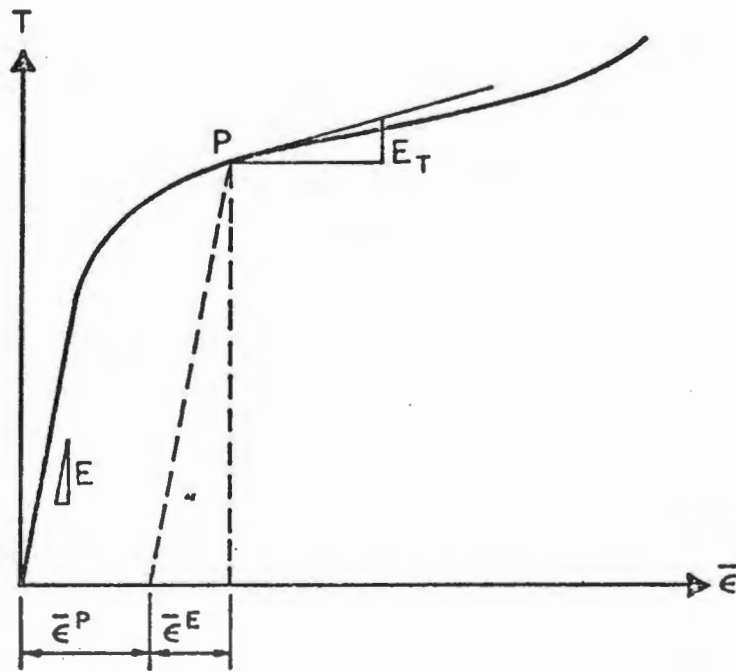


FIG. 2 EXPERIMENTAL STRESS-STRAIN CURVE

$$d\epsilon_{ij}^P = A_{ijkl} d\epsilon_{kl} \quad (11)$$

where

$$A_{ijkl} = \frac{9 s_{ij} s_{kl}}{2\bar{\sigma}^2 (H' + 3\mu)} \quad (12)$$

In Eq. 12, μ is Lamé's constant given by

$$\mu = \frac{E}{2(1 + \nu)} \quad (13)$$

where ν is Poisson's ratio.

The incremental stress-strain relationship is now easily obtained as follows:

$$d\sigma'_{ij} = E_{ijkl} (d\epsilon_{kl} - d\epsilon_{kl}^P) = C_{ijkl} d\epsilon_{kl} \quad (14)$$

in which

$$C_{ijkl} = E_{ijkl} - \frac{9\mu s_{ij} s_{kl}}{\bar{\sigma}^2 (H' + 3\mu)} \quad (15)$$

represents the incremental stress-strain relation; it is symmetric in form. E_{ijkl} represents Hooke's law for elastic deformations. Equation 15 is valid between two consecutive plastic states. According to the loading criterion Eq. 3, when

$$\bar{\sigma} < H \quad (16)$$

or

$$\bar{\sigma} = H \text{ and } s_{ij} d\epsilon_{ij} < 0 \quad (17)$$

the last term of Eq. 15 should be neglected and only Hooke's law remains.

A more general incremental relationship may be found in the book by Hill^[7]. The isotropic strain hardening law that has been utilized here has some shortcomings for repeated or cyclic loading because it does not account for the so-called Bauschinger effect. However, an expression similar to Eq. 15 based on the kinematic hardening law can also be obtained without much difficulty.

Reduction to Plane Stress

Having the application to plates in mind, the special case will be considered in which

$$\sigma_{i3} = d\sigma_{i3} = 0 \quad i = 1, 2, 3 \quad (18)$$

SECTION III

FINITE ELEMENT EQUATIONS

General Incremental Stiffness Matrix

The principle of virtual work can be derived directly from the equilibrium equations for a solid and is valid regardless of material behavior. By applying this principle to a finite element, the following work equation arises

$$du_1^T S_1 = \int_V d\epsilon^T \sigma dV \quad (25)$$

where S_1 and u_1 are the nodal forces and the corresponding displacements. ϵ and σ are the strains and stresses over the volume of the element.

Two configurations of the body during deformation, denoted 1 and 2, will now be considered. Assuming that these two configurations are "close" to each other and writing the virtual work expression for each configuration, the following incremental equation is obtained by subtraction

$$\Delta S_1 = k_I \Delta u_1 \quad (26)$$

where

$$\Delta S_1 = S_1^2 - S_1^1 \quad (27)$$

$$\Delta u_1 = u_1^2 - u_1^1 \quad (28)$$

The incremental stiffness matrix in Eq. 26 is expressed as follows,

$$k_I = \int_V B^T C_{\Delta} B dV \quad (29)$$

in which the strain interpolation matrix B defines the relation between nodal displacements and internal strains

$$\epsilon = B u_1 \quad (30)$$

Note that small displacements are assumed, so that the same strain matrix applies to both configurations. The matrix C_{Δ} represents the stress-strain relationship for the increment between Configurations 1 and 2. In general, the numerical value of C_{Δ} will not be known because it depends on the stress path from 1 to 2, thus an approximate value will have to be used in numerical computations. The simplest approximation would be the value of C at Configuration 1; better accuracy but at the cost of greater computing effort would result from a "mean value" found by a higher order computational scheme.

Incremental Plate Stiffness

By introducing the usual restrictions on the displacement field, as stated in the Kirchhoff theory for plate bending, and making use of the incremental relationship between plane stress and strain described above, the incremental stiffness matrix can be specialized for a plate element. The Kirchhoff hypothesis limits the strains to only three components, ϵ_x , ϵ_y , γ_{xy} , which vary linearly through the thickness. The coordinate system used is shown in Fig. 3.

The displacements will now be separated into two groups: the in-plane displacements defined by

$$v = \begin{Bmatrix} u \\ v \end{Bmatrix} = \phi_v v_i \quad (31)$$

and the out-of-plane displacement

$$w = \phi_w w_i \quad (32)$$

where ϕ_v and ϕ_w are the interpolation polynomials and v_i and w_i are associated nodal point parameters. By appropriate differentiation of these equations, the strains can now be found, expressed in terms of two strain interpolation matrices B_v and B_w , as follows.

$$\epsilon = \begin{Bmatrix} \epsilon_x \\ \epsilon_y \\ \gamma_{xy} \end{Bmatrix} = \begin{bmatrix} B_v & | & zB_w \end{bmatrix} \begin{Bmatrix} v_i \\ \dots \\ w_i \end{Bmatrix} \quad (33)$$

Hence, a partitioned incremental stiffness matrix for the plate is obtained by substitution into Eq. 29.

$$k_I = \begin{bmatrix} k_v & | & k_{vw} \\ \hline k_{vw}^T & | & k_w \end{bmatrix} \quad (34)$$

in which the submatrices

$$k_v = \int_V B_v^T D_\Delta B_v dV = \int_A B_v^T D_{11} B_v dA \quad (35)$$

$$k_{vw} = \int_V z B_v^T D_\Delta B_w dV = \int_A B_v^T D_{12} B_w dA \quad (36)$$

$$k_w = \int_V z^2 B_w^T D_\Delta B_w dV = \int_A B_w^T D_{22} B_w dA \quad (37)$$

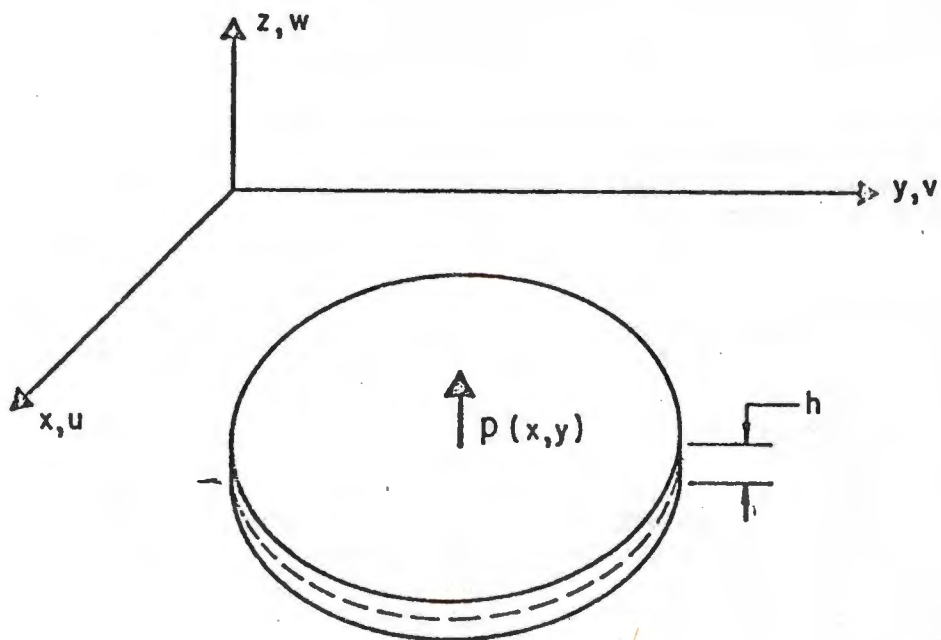


FIG. 3 DESCRIPTION OF THE PLATE IN A CARTESIAN COORDINATE SYSTEM

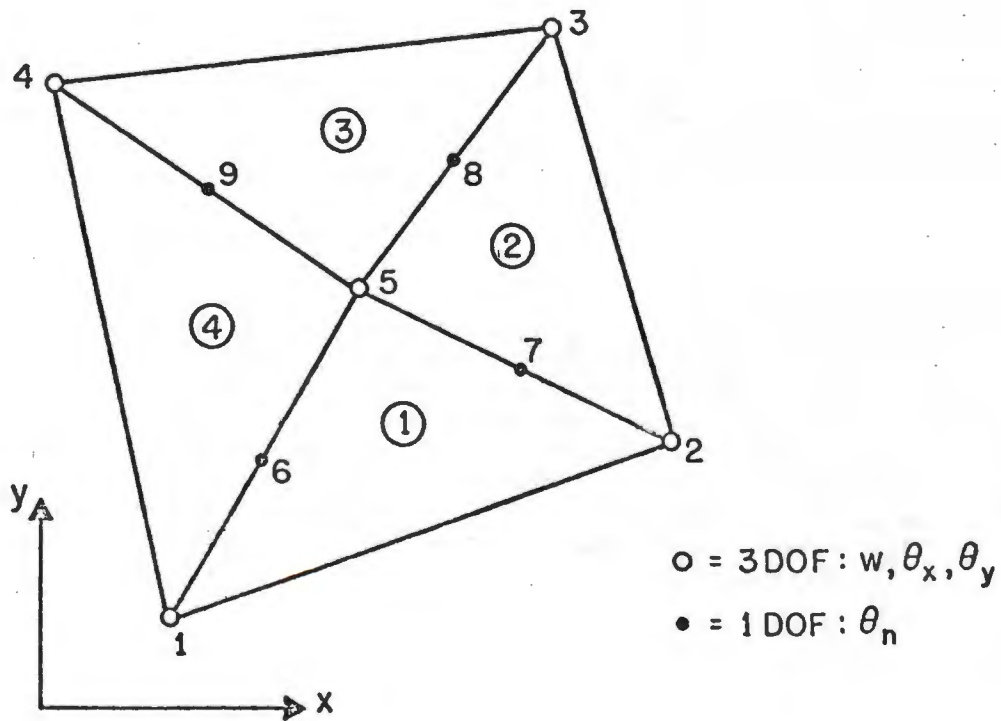


FIG. 4 THE Q19 QUADRILATERAL

represent the in-plane, coupled, and out-of-plane behavior, respectively. D_{Δ} is the incremental constitutive equation for plane stress defined in Eq. 21. Thus it is seen that the plate "constitutive relations" are obtained by integration through the plate thickness

$$D_{11} = \int_{-h}^h D_{\Delta} dz, \quad D_{12} = \int_{-h}^h z D_{\Delta} dz, \quad D_{22} = \int_{-h}^h z^2 D_{\Delta} dz \quad (38)$$

Out-of-Plane Interpolation Functions

The Q-19 plate bending interpolation functions that have been adopted here already have been described completely^[8], and only the main concepts of their development need be repeated for the present purpose. As is shown in Fig. 4, the Q-19 quadrilateral element is assembled from four triangle elements; the coordinates of node 5 of the quadrilateral are the averages of the coordinate of the corner nodes. An element similar to these triangles, an LCCT-12 (linear curvature compatible triangle with 12 DOF) is shown in more detail in Fig. 5. This triangle is divided into three subdomains, each having complete cubic polynomial expansions expressed by natural (triangular) coordinates for the entire triangle. By matching the deflections and rotations for all three subtriangles at the centroid O and enforcing continuity of slopes between these subtriangles at their midside points, all internal DOF can be eliminated. This is a tedious algebraic operation, but the resulting interpolation polynomial, which is stated completely in Reference 8, is quite simple.

The LCCT-12 bending triangle with 12 DOF can easily be reduced to an LCCT-11 triangle by prescribing a kinematic constraint such that the rotation at one midside point is set equal to the arithmetic average of the corresponding slopes at the adjacent corner nodal points. This results in a slight modification of the interpolation polynomials of the LCCT-12 element.

In-Plane Interpolation Functions

A set of in-plane displacement functions defined over a general quadrilateral domain will be needed to develop a "membrane" element consistent with the "bending" element. Only two in-plane DOF's at each corner will be used here for the sake of simplicity. An isoparametric element of this type has been described by Zienkiewicz^[9]. The present element has been improved somewhat by including two internal interpolation functions associated with the displacements at the midpoint and then condensing out these internal DOF's. The displacement functions of this element are expressed in the natural quadrilateral coordinates.

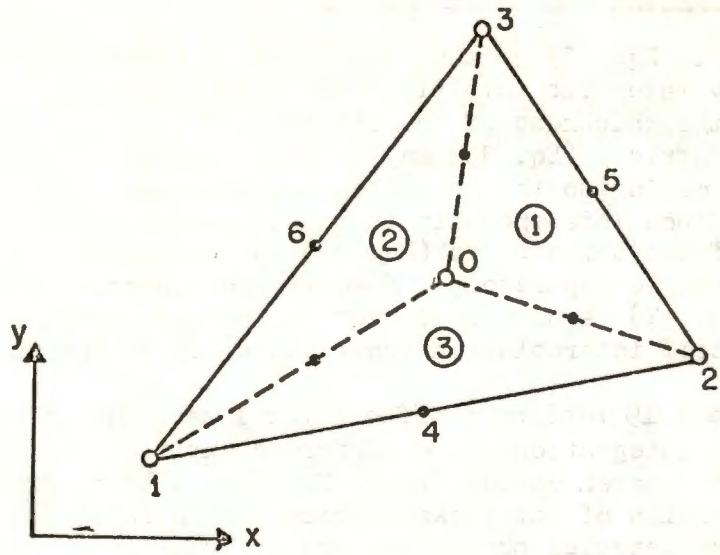


FIG. 5 THE LCCT 12 ELEMENT

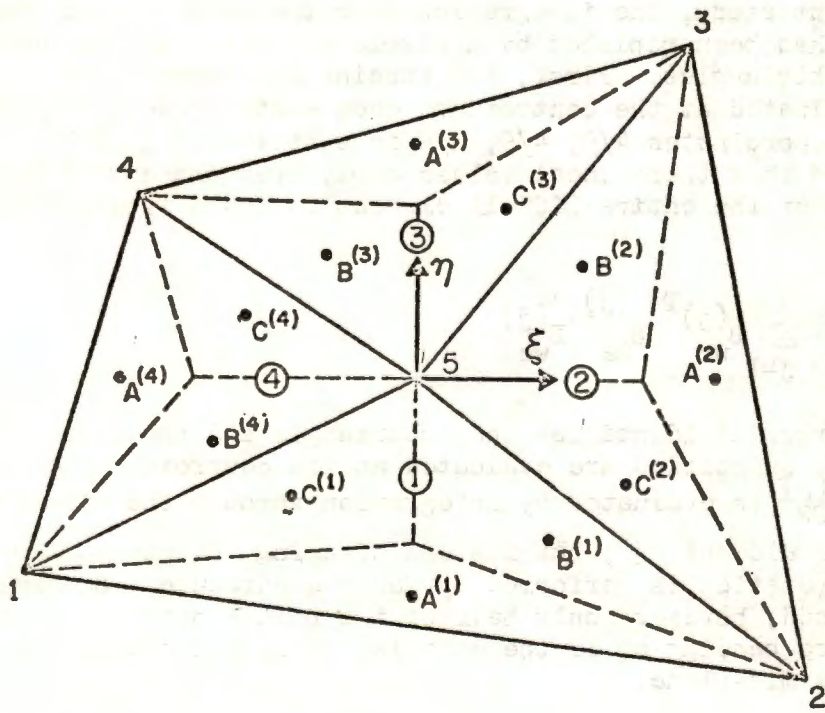


FIG. 6 INTEGRATION POINTS FOR ELASTIC-PLASTIC PLATE BENDING ELEMENT

Numerical Integration of the Element Stiffness

It will be noted in Eqs. 35-38 that the plate stiffness matrix is computed by evaluating integrals involving the constitutive relations, over the area and through the thickness of the element. The integration of the bending stiffness submatrices (Eq. 35) may be done separately for each of the four triangular areas making up the quadrilateral, because the LCCT strain interpolations are defined independently in each. Similarly, for the coupled membrane-bending stiffness submatrices (Eq. 36) the integrations may be performed for each triangle separately. However, the integration of the in-plane stiffness (Eq. 37) is performed over the entire quadrilateral because the isoparametric interpolation functions apply to the full region.

In developing the Q-19 bending stiffness for linear elastic materials, the area and thickness integrations were performed explicitly, the area integration being done in area coordinates. However, a basic problem arises in the explicit integration of stiffness matrices which represent non-linear material behavior: the material properties are not uniform throughout the element volume. In some non-linear finite element analyses, the variation of properties within the element has been expressed by additional interpolation functions, thus making explicit integration possible^[14]. However, this approach would be extremely complicated if applied with the Q-19 interpolation functions described above. Moreover, the incremental stress-strain relationship frequently is a discontinuous function within the element.

In the present study, the integration over the area of each LCCT-11 bending triangle has been replaced by a simple summation of the contributions from its three subtriangles. First, the strains and incremental constitutive relations are evaluated at the centroid of each subtriangle (defined, for example, by area coordinates $4/9, 4/9, 1/9$ in subtriangle 3 of Fig. 5). Then it is assumed that these local values apply over the entire subtriangle, and the stiffness of the entire LCCT-11 element is found from the following expression

$$k_{wt} = \frac{A}{3} \sum_{j=1}^3 B_{wc}^{(j)T} D_{22}^{(j)} B_{wc}^{(j)} \quad (39)$$

in which the superscript identifies the subtriangle and the subscript c indicates that the quantities are evaluated at its centroid. The constitutive relation matrix $D_{22}^{(j)}$ is evaluated by integration through the element thickness at the centroid of element "j", but instead of using the explicit expression of Eq. 38 the computation is performed by Gauss quadrature. Generally an 11-point scheme is used; however, only half of the points need be considered in the case of pure bending or if the material is linear elastic because of symmetry about the mid-plane.

The stiffness k_w of the complete Q-19 element is formed by assembling the four LCCT-11 triangles. If there is no coupling stiffness, the internal

DOF may be condensed out at this stage resulting in a 12 DOF quadrilateral. Although this integration scheme appears quite crude, it is surprisingly effective because each quadrilateral is represented by 12 sub-areas. As a demonstration of the element efficiency, a square simply supported plate subjected to uniform pressure was analyzed using a 2 by 2 quadrilateral mesh for one quarter of the plate. The central deflection obtained from the numerically integrated elements was only 0.4 percent greater than that given by elements integrated exactly.

The in-plane stiffness of an isoparametric quadrilateral element generally is integrated numerically by Gauss quadrature, using a 2 by 2 or a 3 by 3 system of integration points over the area. This integration scheme could be used with non-linear material properties, as well as for the linear elastic case. However, in order to evaluate the coupled stiffness submatrices in the present study, it is necessary to evaluate the in-plane strain interpolations at the same integration points associated with the bending interpolations. Therefore, the in-plane stiffness also is calculated using the same 12 integration points and the same type of summation scheme described for the Q-19 element. In this case, the contributions from the 12 subtriangles may be superposed directly, thus the in-plane stiffness for the entire quadrilateral is given by:

$$k_v = \sum_{m=1}^{12} A^{(m)} B_{vc}^{(m)T} D_{11}^{(m)} B_{vc}^{(m)} \quad (40)$$

in which $A^{(m)}$ represents the area of subtriangle m , and the strain interpolations are evaluated at the subtriangle centroids. As in the bending analysis, the constitutive relation $D_{11}^{(m)}$ is evaluated numerically at the centroid by Gauss quadrature through the thickness. However in this case only a single point is needed (at mid-depth) unless both non-linear materials and combined membrane-bending conditions are involved.

One difficulty is encountered in evaluating the in-plane strains at the subtriangle centroids: the isoparametric interpolation functions are expressed in quadrilateral coordinates while the subtriangles are defined in triangular coordinates. However, noting that the midpoint of the Q-19 element is the same as the origin of the ξ - η quadrilateral coordinates, the following relations may be derived between the two natural coordinate systems on triangle 1 (see Fig. 6):

$$\xi = -\zeta_1^{(1)} + \zeta_2^{(1)} ; \quad \eta = -\zeta_1^{(1)} - \zeta_2^{(1)} \quad (41)$$

where $\zeta_1^{(1)}$ and $\zeta_2^{(1)}$ are area coordinates of triangle 1. From these, and the triangular coordinates of the subtriangle centroids, the quadrilateral coordinates of these points may be derived for triangle 1, as follows:

<u>Subtriangle Centroid</u>	<u>Triangle</u>			<u>Isoparametric</u>	
	$\zeta_1^{(1)}$	$\zeta_2^{(1)}$	$\zeta_3^{(1)}$	ξ	η
A ⁽¹⁾	4/9	4/9	1/9	0	-8/9
B ⁽¹⁾	1/9	4/9	4/9	1/3	-5/9
C ⁽¹⁾	4/9	1/9	4/9	-1/3	-5/9

Similar relations are easily obtainable for triangles 2, 3, and 4.

The coupling stiffness submatrix (Eq. 36) will exist only when the element has non-linear material properties and it is subjected to both flexural and in-plane deformations. The stiffness contribution of each triangular area of the element is obtained from the membrane and bending strain interpolations evaluated at the three subtriangle centroids, using the formula

$$k_{vwt} = \frac{A}{3} \sum_{i=1}^3 B_{vc}^{(j)T} D_{12} B_{wc}^{(j)} \quad (43)$$

in which the notation is similar to Eq. 40. The constitutive relation matrix $D_{12}^{(j)}$ is evaluated by integrating the expression of Eq. 38 using 11 point Gauss quadrature. In the case when $D_{12}^{(j)}$ is non-zero, the corresponding expressions for $D_{11}^{(j)}$ and $D_{22}^{(j)}$ also require the use of all 11 points in their integration.

The stiffness k_{vw} of the complete quadrilateral is obtained by assembling the results given by Eq. 43 for the four triangular areas. Then the system of four submatrices shown in Eq. 34 (which has dimensions 27 x 27) may be reduced to a 20 DOF stiffness matrix by condensing out the seven internal DOF. The result represents the incremental coupled membrane-bending stiffness matrix of the quadrilateral element.

SECTION IV

EXAMPLES

Computer Program

A Fortran IV computer program was developed according to the previous derivations. The main equations associated with this new non-linear capability are those of the plasticity theory, Eqs. 1, 12, 15 and 17, and the stiffness relations, Eqs. 39, 43 and 45. Other operations are the standard ones for the finite element method.

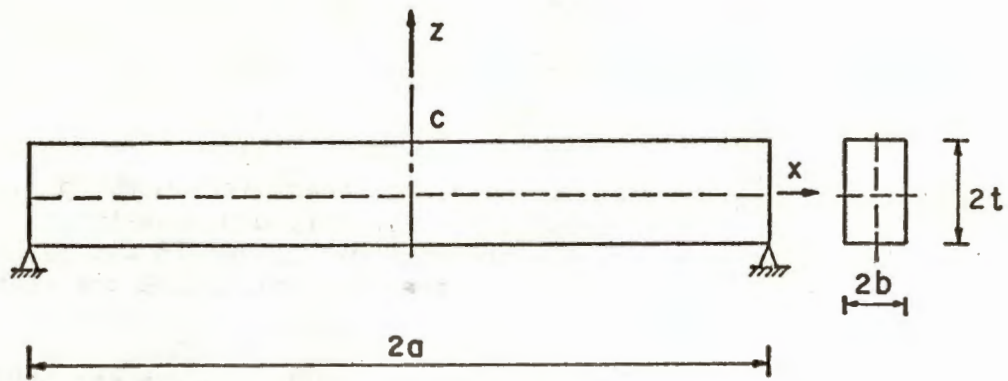
In this program the strain-displacement relationships are computed once only and retained during application of the entire sequence of incremental loads. The initial load is automatically scaled so that initial yielding is obtained at the integration point having the highest equivalent stress. The experimental stress-strain curve is identified in the input by a set of discretized values; linear interpolation is performed for intermediate points. If a new state of stress lies outside the current yield surface according to the $\sigma - \epsilon$ diagram (due to the error of increment linearization), the stresses are scaled linearly back to the yield surface.

A few examples are presented in the following to illustrate the capacity of this formulation. The non-linear solutions are based on a simple Euler-Cauchy incremental technique. This method has certain advantages from a computational point of view because stress-computation and stiffness formulation can be performed simultaneously.

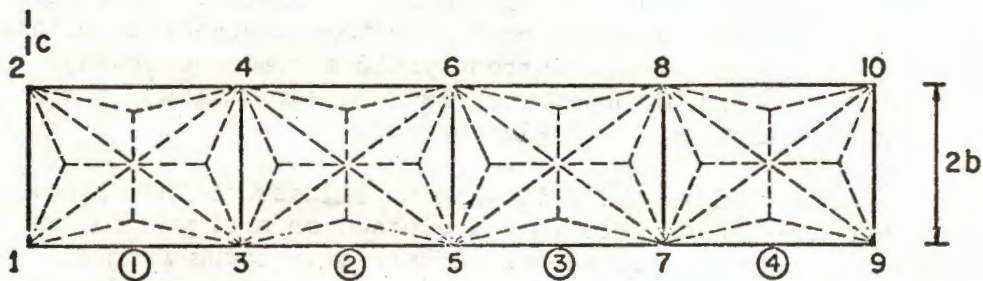
Simple Beam

The first example deals with the bending of a simply supported, rectangular beam subjected to uniform loading. In order to demonstrate both the bending and the membrane capabilities of this element, two different analyses were performed - one involving out-of-plane loading, the other loaded in-plane. The dimensions of the beam and the two finite element idealizations used are shown in Fig. 7.

The results of the two analyses in which the material was assumed to be elastic, perfectly plastic are plotted in Fig. 8. In this figure, the abscissa ρ is a non-dimensional loading factor for which the unit value corresponds to full yielding. The ordinate represents the ratio of the current value of mid-point deflection to the value at initial yielding. For comparative purposes, the results of a closed form solution presented by Prager and Hodge^[15] also are plotted in the figure. The good elasto-plastic performance given by only four bending elements is evident. On the other hand, 20 membrane elements (neglecting symmetry) were required to obtain similar accuracy because these elements are not well adapted to representing bending. Figure 8 also shows



GEOMETRY OF BEAM



$b = 1$
 $a = 20$
 $t = 1$

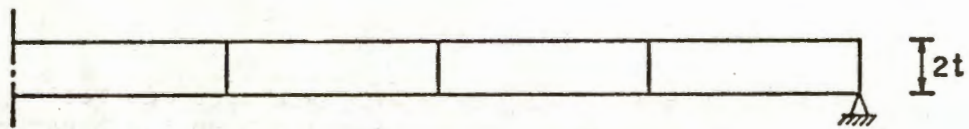
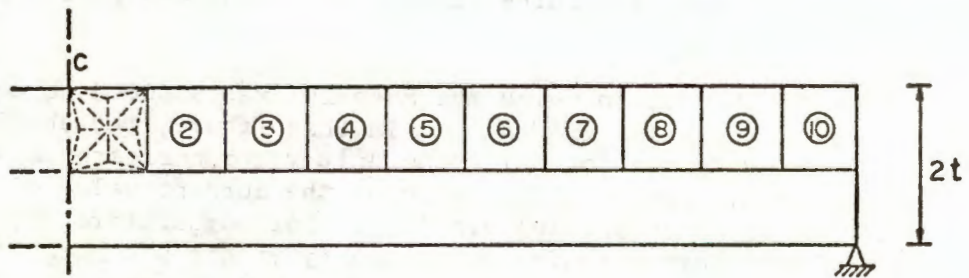


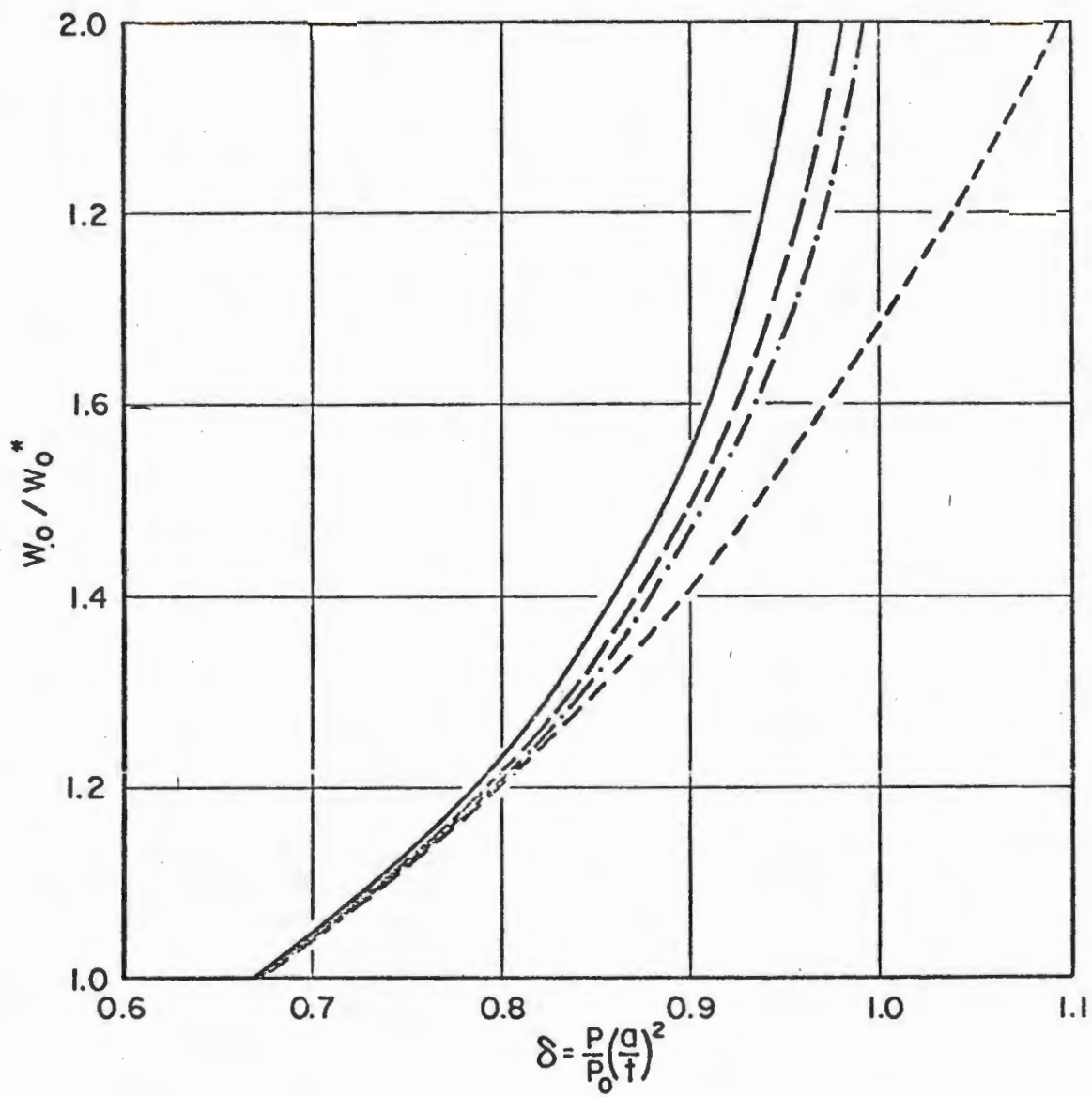
PLATE BENDING ELEMENT IDEALIZATION (1/2 BEAM)



$b = 0.25$
 $a = 10$
 $t = 1$

MEMBRANE ELEMENT IDEALIZATION (1/4 BEAM)

FIG. 7 FINITE ELEMENT IDEALIZATION FOR ELASTIC PLASTIC BEAM



- = PRAGER AND HODGE
- · - · - · = 4 PLATE BENDING ELEMENTS
- = 10 MEMBRANE ELEMENTS
- = 4 PLATE BENDING ELEMENTS, $E_T = 0.25 E$

FIG. 8 ELASTIC - PLASTIC BENDING OF BEAM

results obtained with the plate bending elements, when a bilinear material property is assumed for the beam for which $E_T = 1/4 E$ after yielding.

Square Plate

Figure 9 shows a square, simply supported plate made of an elastic, perfectly plastic material. One quarter of the plate has been idealized by 2 by 2 and by 4 by 4 meshes. A graph of the mid-point deflection due to a uniform pressure also is shown in the figure. The maximum deflection obtained in this analysis can be compared with a yield line, "ultimate load" analysis and an upper bound analysis given by Armen, et al^[4].

Zones having three different depths of yielding through the thickness, due to a loading factor of $\rho = 0.99$, are indicated by different shading patterns in Fig. 10. The development of an incipient yield line mechanism along the diagonal of the plate is evident.

Trapezoidal Plate

The last results to be discussed are those obtained for the plate of trapezoidal shape, Fig. 11, subjected to uniform pressure. Again the material was assumed to be elastic, perfectly plastic. One half of the plate was idealized by a 4 by 4 mesh, and the pressure was applied in increments equal to 10 percent of the initial yield load. The deflection of the midpoint of the free edge through 25 load increments is plotted in Fig. 12. The deflected shape of the free edge at two different load levels, and the yield line theory shape are sketched in Fig. 13; these curves show how the yielding process gradually changes the deflection patterns. The extent of the yielding determined at three different pressure levels are shown in Figs. 14, 15 and 16, which give some idea of the propagation of the yield zones during loading.

Further details concerning these and several other examples may be found in Ref. 12.

Computer Time Requirements

All computations in the preceding examples were made with a CDC 6400 computer (65K memory). The computer time requirements for forming the element stiffness for one quadrilateral element consisting of 12 subregions are indicated in the following tabulation.

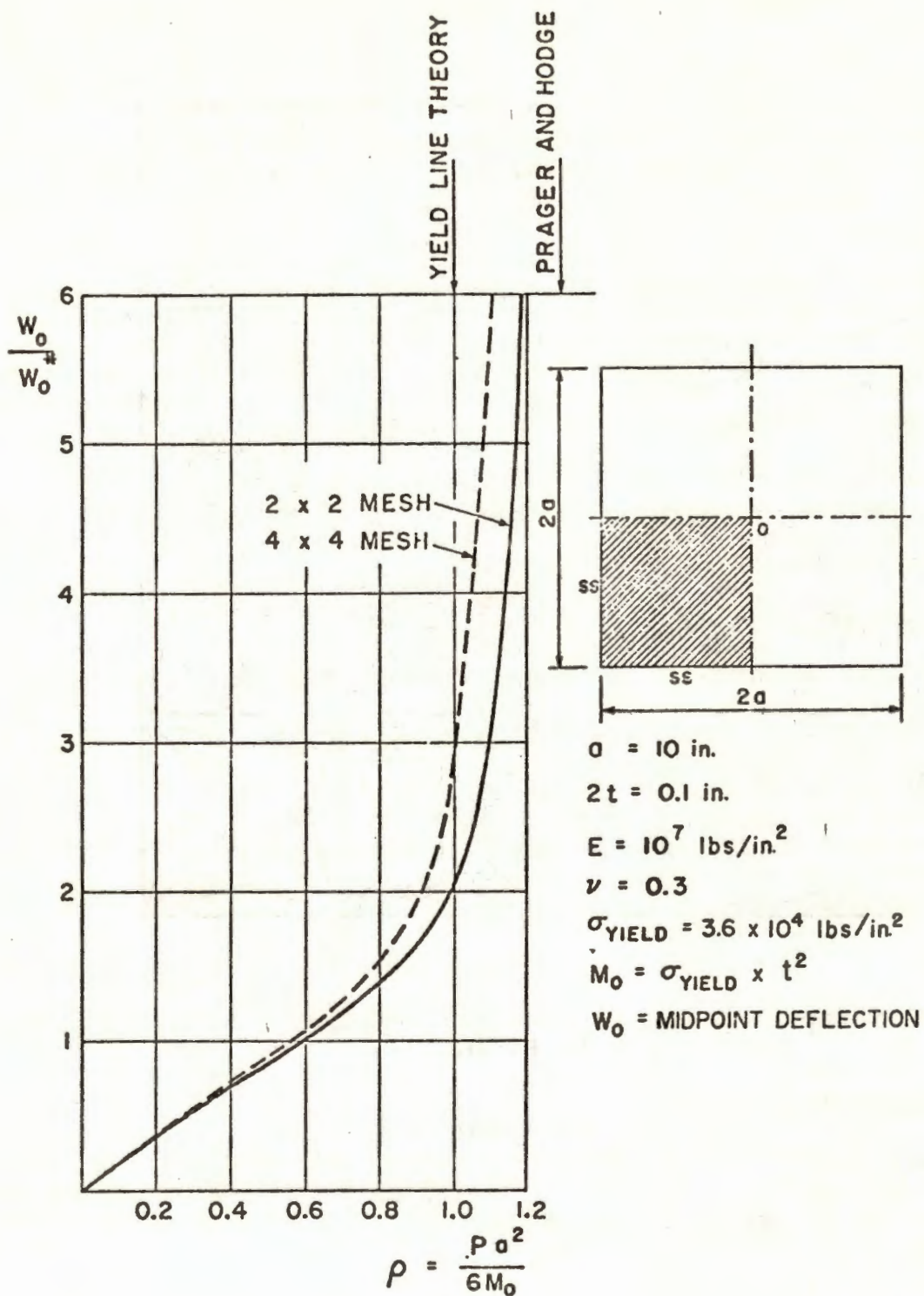


FIG. 9 LOAD DEFLECTION CURVE FOR SIMPLY SUPPORTED SQUARE PLATE

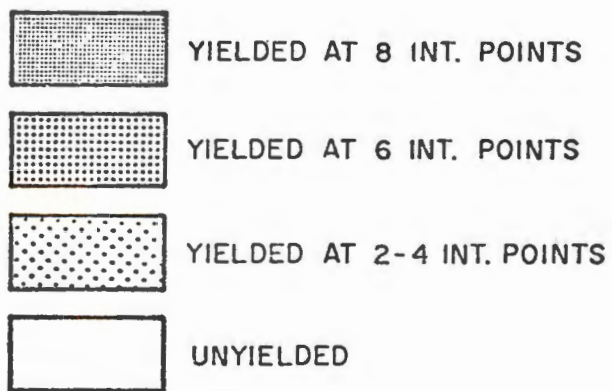
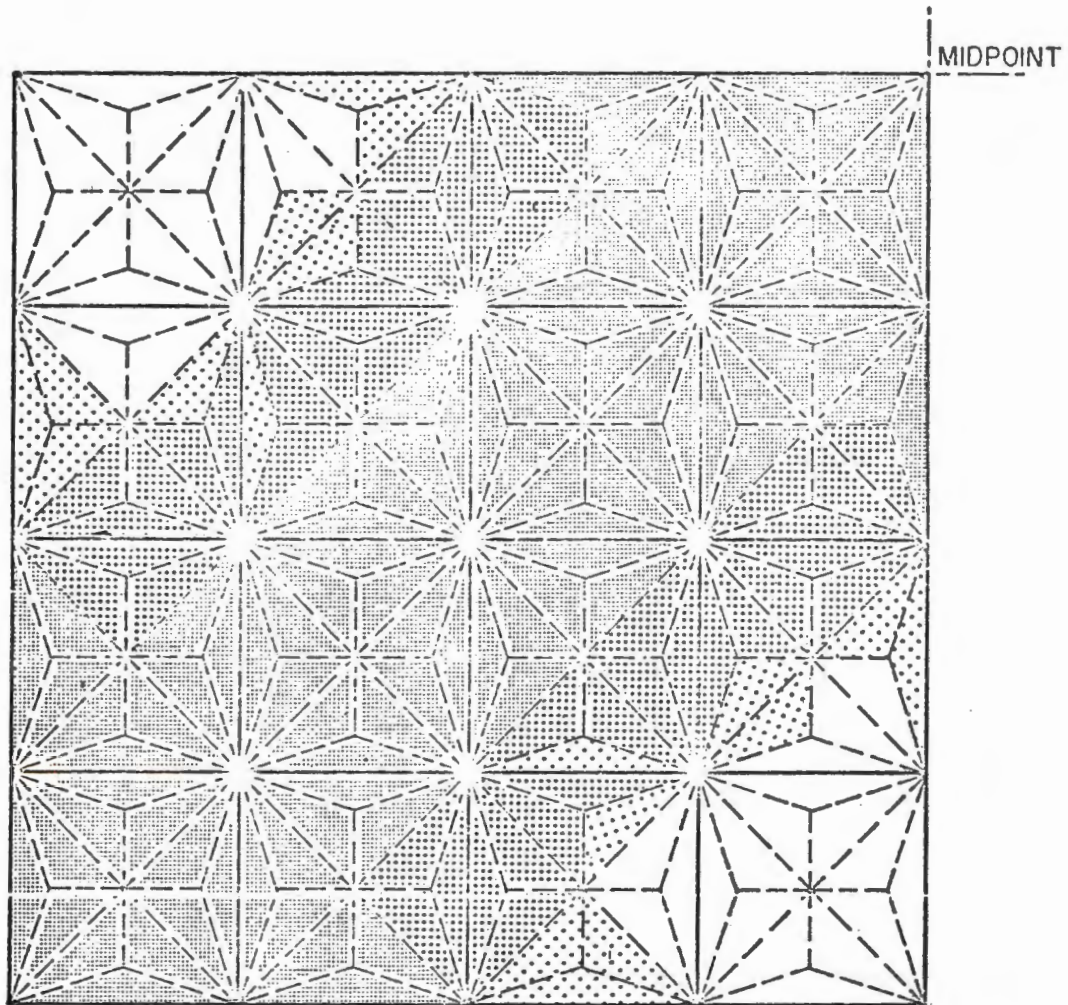


FIG. 10 EXTENSION OF YIELD ZONES FOR $\rho = 0.99$
4 by 4 MESH

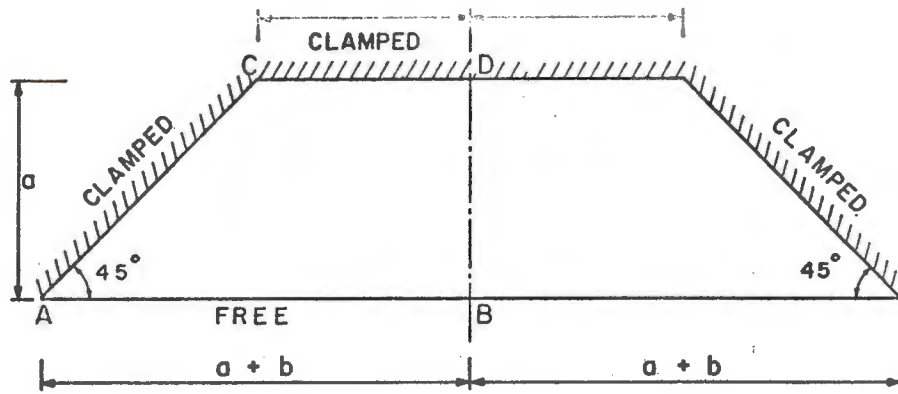


FIG. II TRAPEZOIDAL PLATE

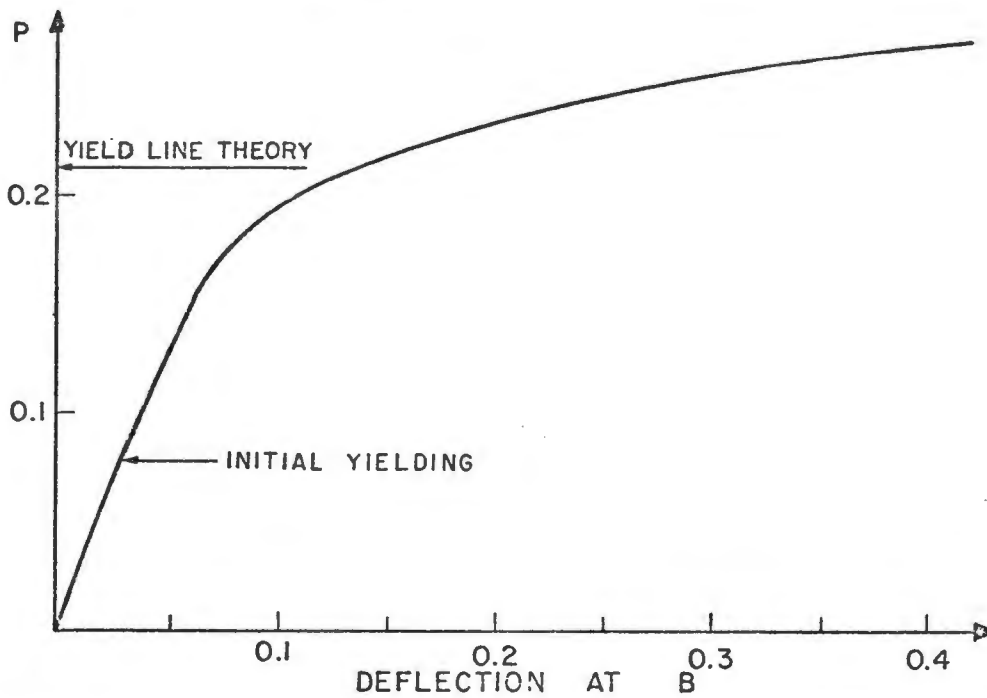


FIG. 12 LOAD-DEFLECTION CURVE FOR TRAPEZOIDAL PLATE

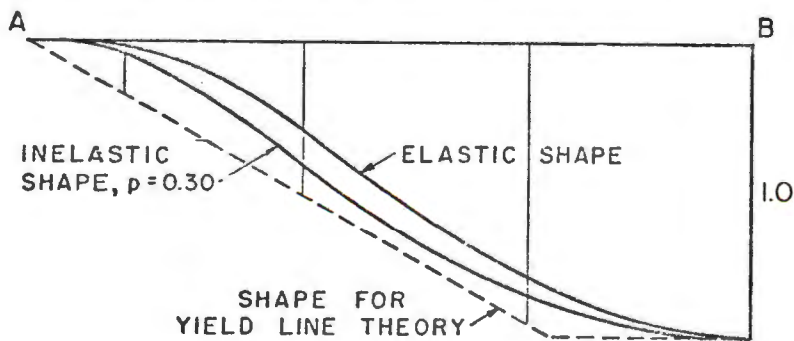


FIG. 13 CHANGES IN DEFLECTED SHAPE ALONG LINE A-B

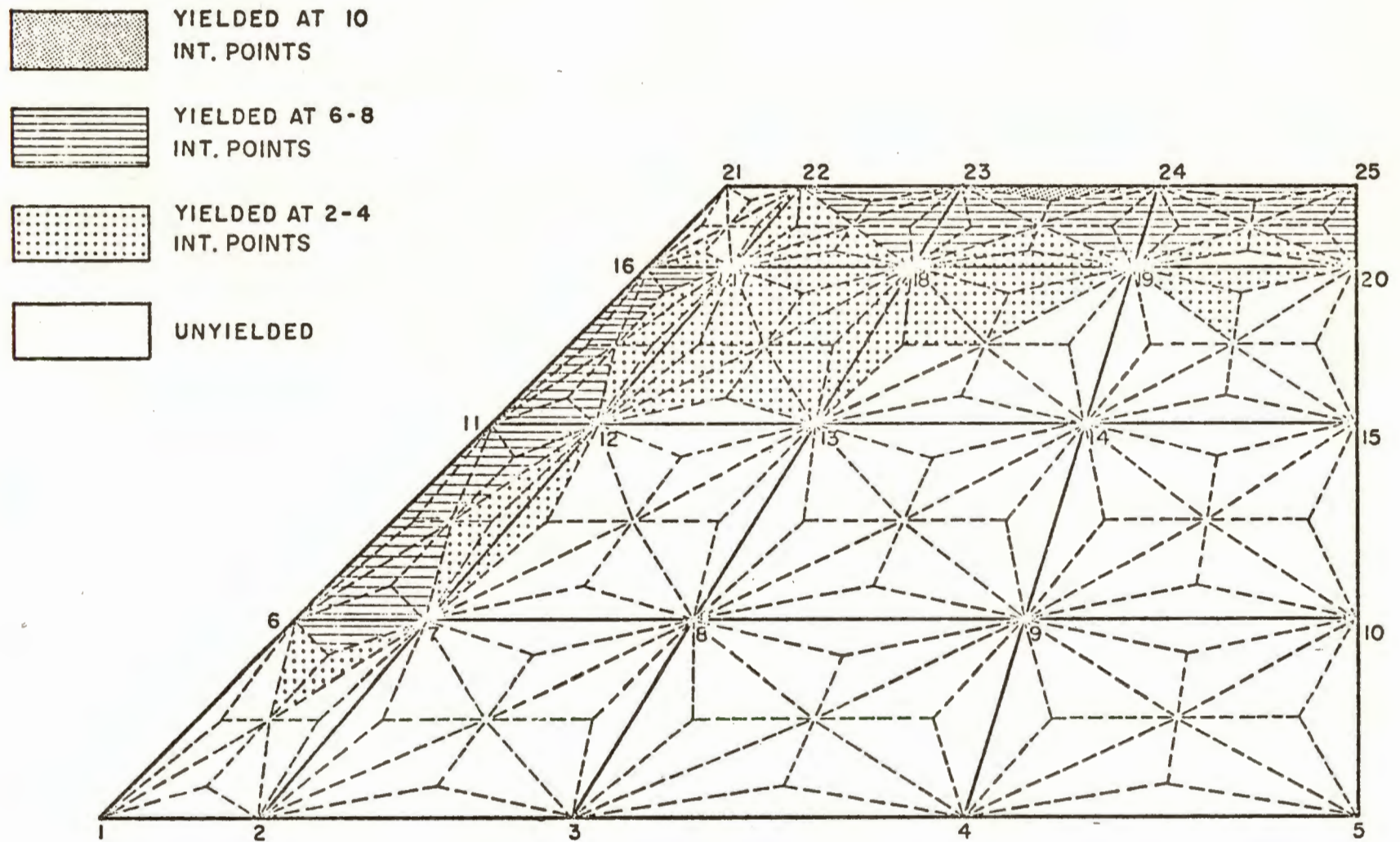


FIG. 14 EXTENSION OF YIELD ZONES FOR $p = 0.173$ (PSI)

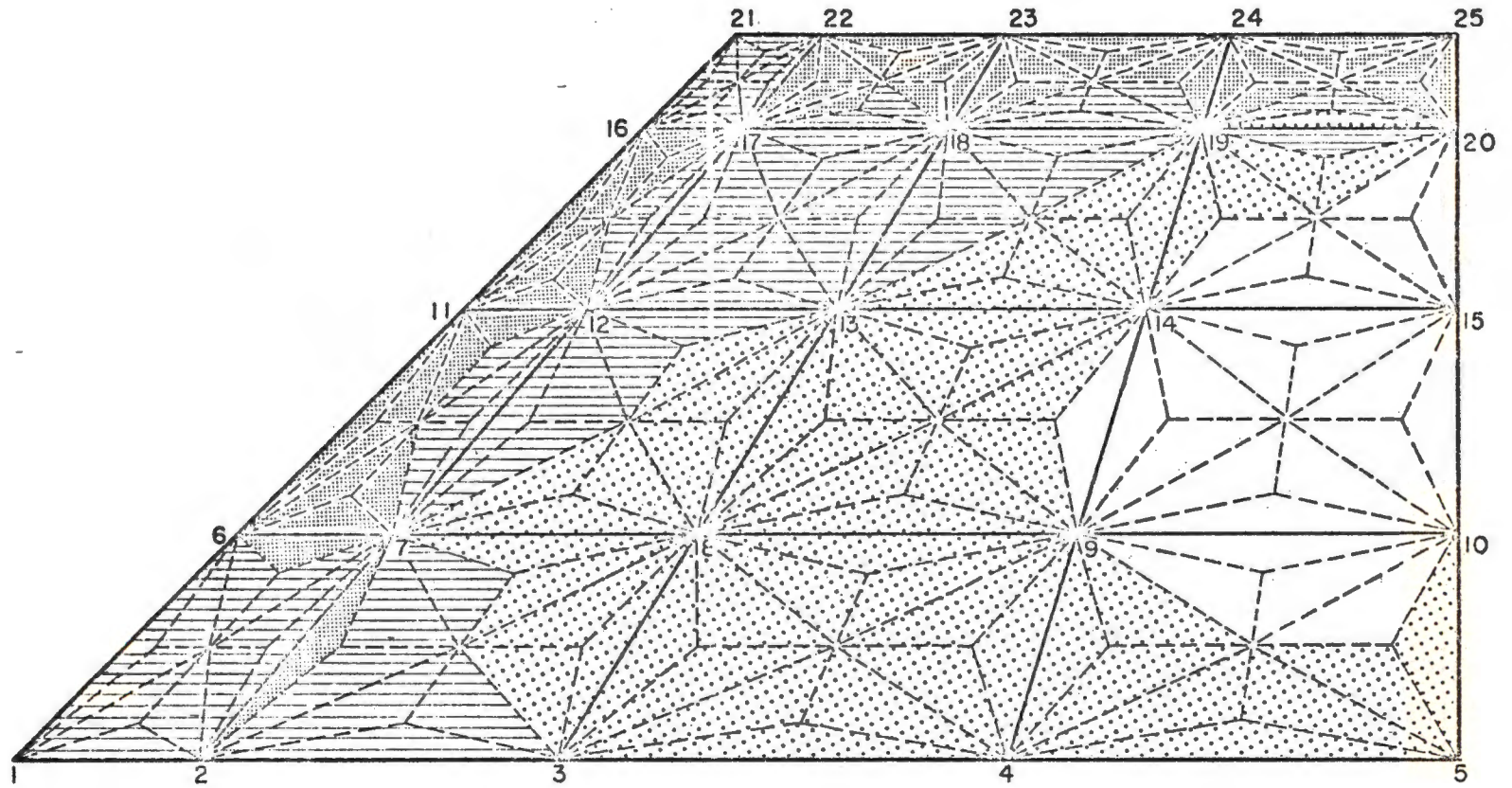


FIG. 15 EXTENSION OF YIELD ZONES FOR $p = 0.221$ (PSI)

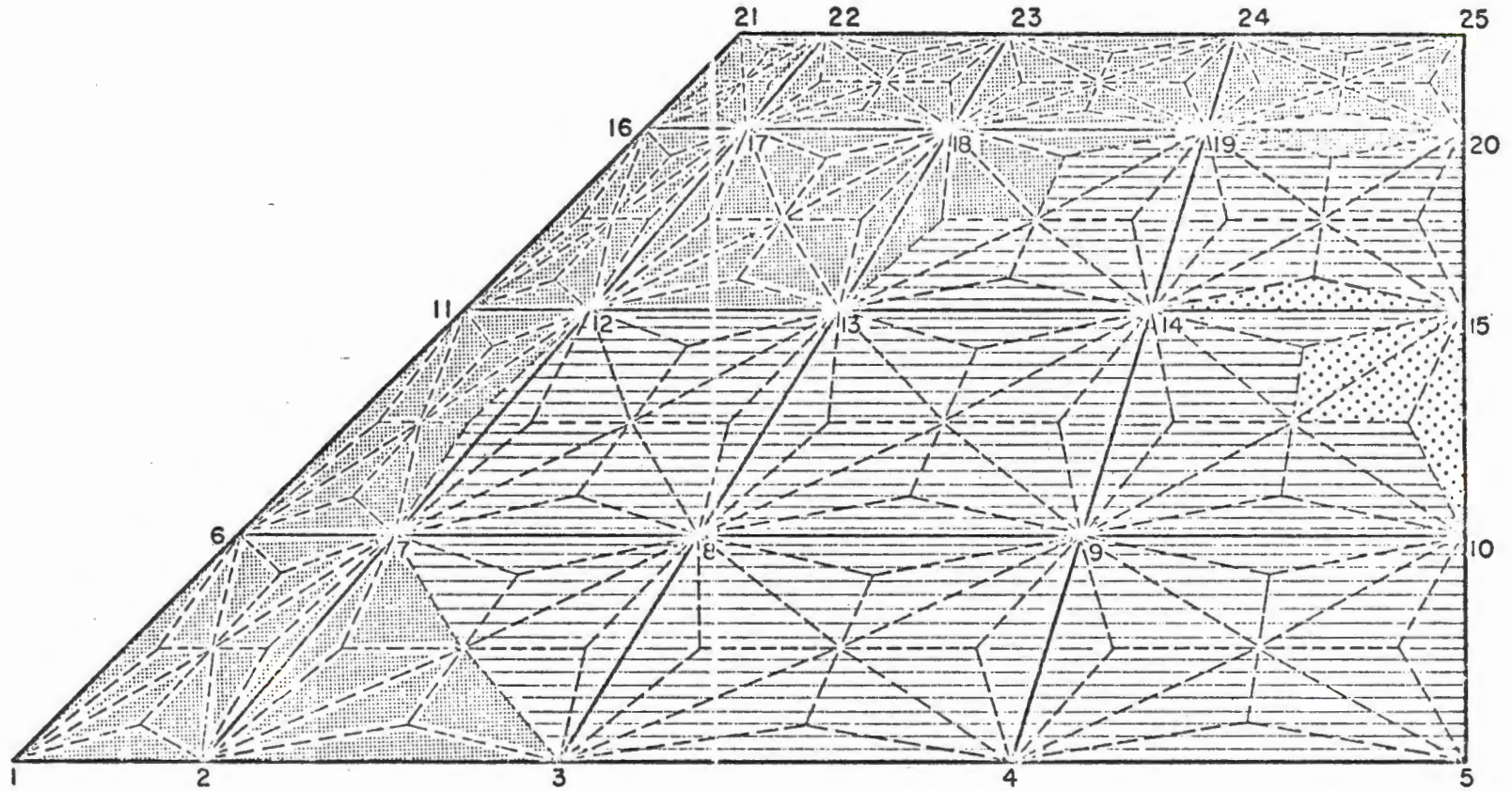


FIG. 16 EXTENSION OF YIELD ZONES FOR $p = 0.268$ (PSI)

Operation	Time CP secs.
Incremental stiffness for inelastic plate bending element, 11 int. points through thickness	0.170 - 0.330
Incremental stiffness for inelastic membrane element	0.125 - 0.160
Incremental stiffness for combined bending and membrane action, 11 int. points through thickness	0.540 - 0.690

The computer time requirements for performing the analyses of some of the previous examples are:

Example	No. of elements	No. of load increments	Time CP secs.
Inelastic beam, bending element	4	19	24
Inelastic beam, membrane element	10	19	35
Trapezoidal plate	16	29	171

SECTION V

CONCLUSIONS

1. The Q-19 bending element may be combined with the linear isoparametric membrane element to provide an efficient element for treating coupled membrane-bending effects.
2. The area integration required in the element stiffness evaluation may be approximated effectively by summing terms evaluated at the centroids of the 12 subtriangles of the Q-19 element. Thickness integrations are done most efficiently by Gauss quadrature.
3. Non-linear analyses may be accomplished efficiently using simple incremental load analyses based on tangent stiffness defined by the above-mentioned integration processes. Experience shows that large coupled membrane-bending problems can be handled with reasonable expenditures of computer time.

REFERENCES

1. Argyris, J. H., Kelsey, S. and Kamel, H., "Matrix Methods of Structural Analysis - A Precip of Recent Developments," *Agardograph* 72, pp. 1-164, Pergamon Press, 1964.
2. Marcal, P. V., and King, I. P., "Elastic-Plastic Analysis of Two-Dimensional Stress Systems by the Finite Element Method," *Int. J. Mech. Sci.*, Vol. 9, No. 3, pp. 143-145, 1967.
3. Khojasteh-Bakht, M., "Analysis of Elastic-Plastic Shells of Revolution under Axisymmetric Loading by the Finite Element Method," Ph.D. Dissertation, University of California, Berkeley, Report No. SESM 67-8, 1967.
4. Armen, H., Pifko, A., and Levine, H. S., "Finite Element Method for the Plastic Bending Analysis of Structures," *Proc. Second Conf. on Matrix Methods in Struct. Mechanics*, AFFDL-TR-68-150, 1968.
5. Argyris, J. H., and Scharpf, D. W., "Methods of Elasto-plastic Analysis," *Proceedings ISO-ISSC Symposium on Finite Element Techniques at the ISD*, Stuttgart, Germany, 1969.
6. Marcal, P. V., "Finite Element Analysis with Material Nonlinearities-Theory and Practice," *Proc. Japan-U.S. Seminar on Matrix Methods of Structural Analysis and Design*, Tokyo, 1969.
7. Hill, R., The Mathematical Theory of Plasticity, Oxford University Press, 1950.
8. Clough, R. W. and Felippa, C. A., "A Refined Quadrilateral Element for Analysis of Plate Bending," *Proc. Second Conf. on Matrix Methods in Struct. Mech.*, AFFDL-TR-68-150, pp. 399-440, 1968.
9. Zienkiewicz, O. C., The Finite Element Method in Structural and Continuum Mechanics, McGraw-Hill Publ. Company, 1967.

10. Marcal, P. V., "Comparative Study of Numerical Methods of Elastic-Plastic Analysis," AIAA Journal, Vol. 6, No. 1, pp. 157-158, 1967.
11. Naghdi, P. M., "Stress-Strain Relations in Plasticity and Thermoplasticity," Plasticity, Proceedings of the Second Symposium on Naval Structural Mechanics, (editors: Lee, E. H. and Symonds, P. S.), Pergamon Press, 1960
12. Bergan, P. G., "Nonlinear Analysis of Plates Considering Geometric and Material Effects," Ph.D. Dissertation, University of California, Berkeley, March, 1971.
13. Yamada, Y., "Recent Japanese Developments in Matrix Displacement Method for Elastic-Plastic Problems," Proc. Japan-U.S. Seminar on Matrix Methods of Structural Analysis and Design, Tokyo, 1969.
14. Felippa, C. A., "Refined Finite Element Analysis of Linear and Nonlinear Two-Dimensional Structures," Ph.D. Dissertation, University of California, Berkeley; first part published as SESM Report 66-22, 1966.
15. Prager, W. and Hodge, P. G., Theory of Perfectly Plastic Solids, Dover Publications, New York, 1951.